ChemComm

COMMUNICATION

View Article Online
View Journal | View Issue

Cite this: *Chem. Commun.*, 2015, **51**, 3162

Received 24th November 2014,
Accepted 9th January 2015

DOI: 10.1039/c4cc09381j

www.rsc.org/chemcomm

Graphite sulphate – a precursor to graphene†

Siegfried Eigler

Graphite sulphate is used as a precursor to graphene for the first time. The positively charged graphene layers react with water to yield a processable graphene derivative. The unprecedented low density of defects is determined to be 0.06% on average and may open the way for electronic applications.

Graphene is a nanomaterial of interdisciplinary interest and attracts attention of physicists as well as chemists or engineers.[1–3] Chemical vapour deposition is currently the method of choice to prepare large area graphene films and the quality is constantly increasing.[4] However, the wet-chemical synthesis of graphene is scalable and provides high potential for applications.[5,6]

Recently, the direct exfoliation of graphite in organic solvents attracted a lot of attention.[7,8] Although flakes of graphene (G_1) and few-layer graphene ($G_{\text{few-layer}}$) were wet-chemically produced by non-covalent exfoliation, the size of flakes is <1 μm and solvents with high boiling points are needed that limit the overall quality.[8] Graphene oxide (GO), an oxo-functionalised derivative of graphene, can be prepared on a large scale and mostly single layers with a reasonable size of flakes of several μm are obtained.[6] Furthermore, there is constant progress in improving functionalisation methods.[5,6,9] GO is also a potential precursor of graphene, however, with a variable amount of defects.[10,11] The quality of GO strongly depends on the synthetic protocol. Thus, GO can be amorphous, like humic acids, as a result of CO_2 formation due to over-oxidation, or the carbon framework remains almost intact by avoiding CO_2 formation during synthesis under certain reaction conditions.[6,10,12,13]

Generally, the quality of G_1 is limited by the density of defects within the carbon framework of GO.[11,14,15] Furthermore, defects in G_1 limit its performance in applications, such as electronic devices. Consequently, novel synthetic protocols have to be developed to further limit the formation of defects. The lowest density of defects in GO, reported yet, is about 0.3% on average, as determined by statistical Raman microscopy (SRM).[6,11,16] The lowest density of defects of single flakes of GO is as low as 0.01%. Also the mobility of charge carriers depends on the density of defects of related G_1 and values of about 250 cm^2 V^{-1} s^{-1} are described for a density of defects of 0.3% and 1000 cm^2 V^{-1} s^{-1} for a density of defects of 0.01%.[6,10] However, to enter the field of electronic applications, such as sensor materials or transparent electrodes, the average quality of wet-chemically prepared G_1 must be enhanced. Also strong oxidants, such as potassium permanganate in sulfuric acid, commonly used to synthesise GO, bear some problems.[10,17,18] The reaction is exothermic and must be controlled by cooling and manganese salts are not environmentally friendly. Additionally, manganese impurities in graphene based materials should be avoided because they disturb their properties in applications.[19–21]

Here, it is demonstrated for the first time that processable oxo-functionalised graphene is yielded from graphite sulphate (Scheme 1), which is a precursor to G_1 and $G_{\text{few-layer}}$ with an unprecedented low density of defects of about 0.06% on average with a reasonable size of flakes of about 1–5 μm.

Recently, Dimiev *et al.* published the investigation of the formation of blue stage 1 graphite sulphate from natural graphite in sulphuric acid using persulphate as an oxidant (Scheme 1).[22,23] Although graphite sulphate is well known since decades,[24–27] it was not demonstrated to be a suitable precursor of oxo-functionalised graphene (oxo-G_1) or G_1 with a low density of defects. Rüdorff and Hofmann characterised graphite sulphate in depth,[25] and their analyses revealed an ideal structure of the stage 1 intercalation compound of $C_{24}{}^{+}HSO_4{}^{-}\cdot 2H_2SO_4$ (Scheme 1). It can be assumed that the positively charged G_1 layers in graphite sulphate can react with donors, such as water. However, up to now attempts failed to yield functionalised G_1, with lateral dimensions of several μm, confirmed by Raman spectroscopy.[28,29]

At first, graphite sulphate was prepared by the procedure described by Dimiev *et al.* from natural graphite in sulphuric acid by the addition of persulphate (Scheme 1).[22,23] The formation of graphite sulphate is confirmed by the colour change from black to blue (Fig. S1A, ESI†) and further confirmed by Raman spectroscopy.

Department of Chemistry and Pharmacy and Institute of Advanced Materials and Processes (ZMP), Friedrich-Alexander-Universität Erlangen-Nürnberg (FAU), Dr.-Mack Str. 81, 90762 Fürth, Germany. E-mail: siegfried.eigler@fau.de; Fax: +49 (0)911 6507865015; Tel: +49 (0)911 6507865005

† Electronic supplementary information (ESI) available: Experimental details, AFM images, and Raman investigation. See DOI: 10.1039/c4cc09381j

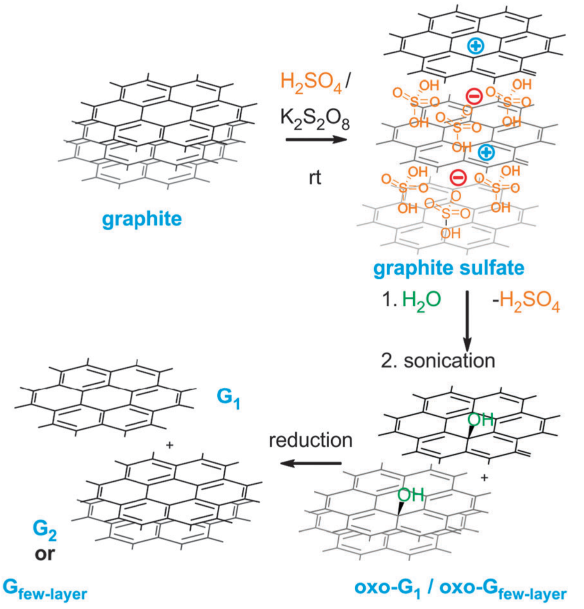

Scheme 1 Synthesis of graphene (G_1) and few-layer graphene ($G_{few-layer}$) by the synthesis of graphite sulphate from natural graphite in sulfuric acid and persulphate under ambient conditions, followed by the reaction with water; sonication yields oxo-G_1 and oxo-$G_{few-layer}$; G_1 and $G_{few-layer}$ are yielded after reduction.

A single Raman band at 1624 cm^{-1} is observed as depicted in Fig. S1B (ESI†). After the formation of graphite sulphate, the reaction mixture was diluted with water, causing an increase in temperature to 60 °C. Excess of sulphuric acid and other salts were removed by repeated centrifugation and redispersion in water. The oxidation of graphite flakes was indicated by Raman spectroscopy by the defect induced broad D peak (Fig. S2, ESI†). Sonication of the oxidised particles in a mixture of water and methanol (1/1) caused exfoliation to oxo-$G_{few-layer}$ and even delamination to oxo-G_1. Larger particles were subsequently removed by centrifugation and the Langmuir–Blodgett technique was used to deposit flakes on a 300 nm SiO_2/Si wafer for analysis by atomic force microscopy (AFM) and SRM. In Fig. 1A the AFM image of oxo-G_1 and oxo-$G_{few-layer}$ is depicted (AFM overview shown in Fig. S3, ESI†). An area of 40.000 μm^2 of the film of flakes was investigated by SRM. The analysis of the disorder induced D peak, the G peak and the 2D peak confirms the absence of any graphene or unoxidised graphitic material as illustrated by the plot of I_D/I_G against Γ_D (Fig. S4, ESI†). Due to the functionalization in oxo-G_1 and oxo-$G_{few-layer}$ $\Gamma_D = 100 \pm 15$ cm^{-1}. The degree of functionalization is roughly estimated to be about 4%, as outlined below and in Table S1 (ESI†). UV/Vis spectra reveal an absorption band at 318 nm beneath 253 nm, which indicates residual unoxidised domains in oxo-G_1 and oxo-$G_{few-layer}$ (Fig. 1B). Furthermore, a C-content of 86% is determined by elemental analysis (EA) and also the mass-loss determined by thermogravimetric analysis (TGA) of 13% indicates the low degree of oxidation (Fig. 1D). An *m/z* 64 is detected which relates to SO_2 formation at a decomposition temperature with a maximum at 380 °C, which originates most likely from organosulphate, as identified before.[30] The residual S-content determined by EA is 1.6% and thus, about 5% of the

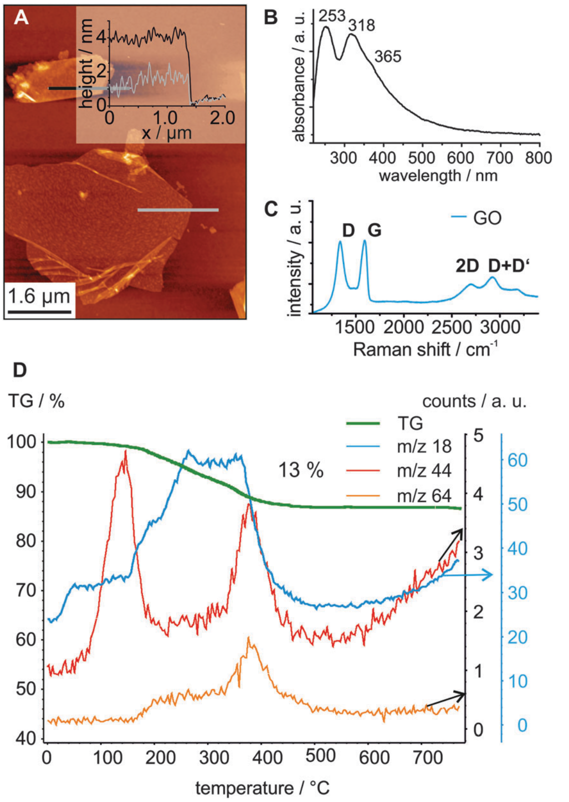

Fig. 1 (A) Atomic force microscope (AFM) image of oxo-G_1 and oxo-$G_{few-layer}$; inset: height-profile along black and grey line. (B) UV/Vis spectrum of oxo-G_1 and oxo-$G_{few-layer}$. (C) Raman spectrum of a typical flake of oxo-G_1. (D) Thermogravimetric analysis of restacked oxo-functionalised graphene and temperature profiles of *m/z* 18, 44 and 64.

mass is related to organosulphate. This observation is in agreement with a recent study on the contamination of GO by chemical treatment.[19] TGA data further reveal that water is the major species detected between 250 °C and 350 °C which contributes mostly to the main weight-loss. A structure containing hydroxyl groups is further supported by FTIR spectroscopy (Fig. S5, ESI†). Consequently, a plausible structure of hydroxylated graphene with trapped water molecules and some organosulphate is proposed (Scheme 1).

Subsequently, the quality of G_1 was determined. Flakes of oxo-G_1 and oxo-$G_{few-layer}$ were deposited on a 300 nm SiO_2/Si wafer and exposed to vapour of hydroiodic acid and trifluoroacetic acid, a highly efficient reduction method suitable to generate G_1.[15] The flakes of G_1 and $G_{few-layer}$ were analyzed by AFM and the images reveal a height of G_1 of about 1 nm (Fig. 2B) and a typical size of flakes of approximately 1–5 µm (Fig. S6, ESI†). The G_1 nature of flakes was confirmed by Raman spectroscopy and the density of defects within the carbon framework of G_1 was also evaluated. Raman spectra of G_1 exhibit a G and 2D peak in addition to a defect induced D peak. The full-width at half-maximum (Γ) of the 2D peak is a criterion to identify single layers of G_1 by a value < 40 cm^{-1}.[31–33] Furthermore, spectra of $G_{few-layer}$ can be filtered by the intensity of the G peak.[16] For the first time, the SRM analysis of data probed from an area of 250.000 μm^2 reveals that 79% of Raman spectra of G_1 (out of 2873 spectra) show a

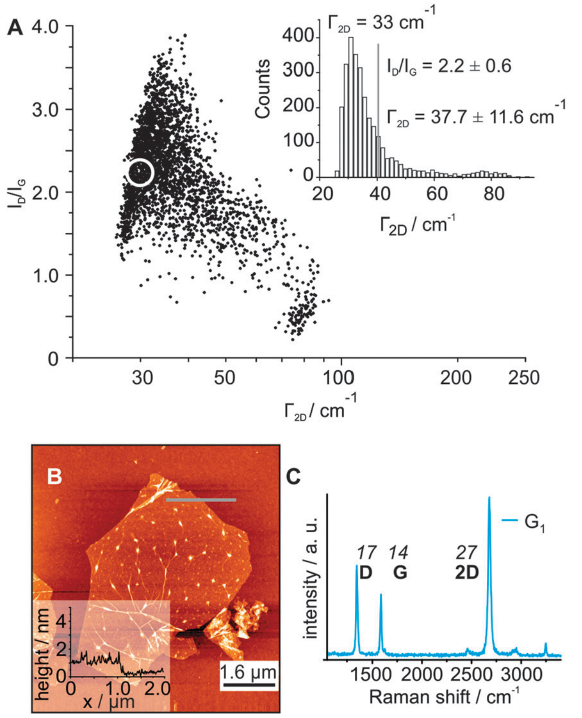

Fig. 2 (A) SRM analysis of a film of flakes of G_1 (plot of I_D/I_G against Γ_{2D}, spectra of $G_{\text{few-layer}}$ filtered by I_G) which indicates the high quality of G_1 by the narrow average Γ_{2D} values of <40 cm^{-1}; inset: histogram of Γ_{2D} with the maximum of Γ_{2D} = 33 cm^{-1}. (B) AFM image of G_1 derived from oxo-G_1; inset: height-profile along the grey line. (C) Raman spectrum of G_1, $\Gamma_{D,G,2D}$ in italic numbers.

Γ_{2D} < 40 cm^{-1} (Fig. 2A). The Γ_{2D} values of analyzed spectra indicate a maximum in the histogram at 33 cm^{-1} depicted in the inset of Fig. 2A. A typical Raman spectrum of G_1 is presented in Fig. 2C with a Γ_{2D} = 27 cm^{-1}. The relation of Raman data and the density of defects was introduced by Lucchese and Cançado and allows estimating the density of defects to about 0.06% on average.[31,34] In comparison, the best average quality of G_1 prepared from GO with an almost intact carbon framework (ai-GO) was 0.3%.[10] The here presented data indicate the best average quality, with a density of defects of 0.06% with a µm size of flakes ($^{1\text{–}5\mu\text{m},0.06\%}G_1$). The reaction of graphite sulphate with water was also conducted at <10 °C, conditions used for the preparation of ai-GO.[10] SRM data reveal a slightly increased quality of G_1 with a density of defects of about 0.04% (Fig. S7, ESI†). Unfortunately, the yield of G_1 prepared here can only be estimated, because of contamination with $G_{\text{few-layer}}$. However, SRM data reveal that about 25% of flakes are G_1 and improvement of separation techniques will increase the part of G_1. Furthermore, the amount of G_1 isolated from 1 g of graphite is on the mg scale but may be suitable for the development of sensor materials.

It can be concluded that the positively charged carbon layers of graphite sulphate can be functionalised under ambient reaction conditions with water as a donor. The multi-layered material readily delaminates in water–methanol to oxo-G_1 and oxo-$G_{\text{few-layer}}$. The degree of functionalization is roughly estimated to be approximately 4% and hydroxyl groups beneath some organosulphate groups are proposed. Although the yield of dispersed G_1 and $G_{\text{few-layer}}$ is improvable, the size of flakes is 1–5 µm, suitable even for applications, such as sensor devices. For the first time, an unprecedented low average density of defects of 0.06% was determined for wet-chemically prepared flakes of G_1 and all Raman spectra of G_1 exhibit a sharp 2D peak. Although the potential of this type of oxo-G_1 is not yet explored, it can be assumed that it is a precursor to G_1 suitable for functionalization. Also the reactivity of G_1 and the influence of defects can be evaluated and the field of electronic applications is within reach.

The author acknowledges the Deutsche Forschungsgemeinschaft for funding *via* grant EI 938/3-1 and thanks Prof. Dr. Andreas Hirsch for his support at FAU Erlangen-Nürnberg. This work is also supported by the Cluster of Excellence 'Engineering of Advanced Materials (EAM)' and SFB 953 funded by the DFG.

Notes and references

1 W. Ren and H. M. Cheng, *Nat. Nanotechnol.*, 2014, **9**, 726–730.
2 A. H. Castro Neto, N. M. R. Peres, K. S. Novoselov and A. K. Geim, *Rev. Mod. Phys.*, 2009, **81**, 109–162.
3 K. S. Novoselov, V. I. Fal'ko, L. Colombo, P. R. Gellert, M. G. Schwab and K. Kim, *Nature*, 2012, **490**, 192–200.
4 Y. Hao, M. S. Bharathi, L. Wang, Y. Liu, H. Chen, S. Nie, X. Wang, H. Chou, C. Tan, B. Fallahazad, H. Ramanarayan, C. W. Magnuson, E. Tutuc, B. I. Yakobson, K. F. McCarty, Y. W. Zhang, P. Kim, J. Hone, L. Colombo and R. S. Ruoff, *Science*, 2013, **342**, 720–723.
5 D. R. Dreyer, A. D. Todd and C. W. Bielawski, *Chem. Soc. Rev.*, 2014, **43**, 5288–5301.
6 S. Eigler and A. Hirsch, *Angew. Chem., Int. Ed.*, 2014, **53**, 7720–7738 (*Angew. Chem.*, 2014, **126**, 7852–7872).
7 Y. Hernandez, V. Nicolosi, M. Lotya, F. Blighe, Z. Sun, S. De, I. T. McGovern, B. Holland, M. Byrne, Y. Gun'Ko, J. Boland, P. Niraj, G. Duesberg, S. Krishnamurti, R. Goodhue, J. Hutchison, V. Scardaci, A. C. Ferrari and J. N. Coleman, *Nat. Nanotechnol.*, 2008, **3**, 563–568.
8 K. R. Paton, E. Varrla, C. Backes, R. J. Smith, U. Khan, A. O'Neill, C. Boland, M. Lotya, O. M. Istrate, P. King, T. Higgins, S. Barwich, P. May, P. Puczkarski, I. Ahmed, M. Moebius, H. Pettersson, E. Long, J. Coelho, S. E. O'Brien, E. K. McGuire, B. M. Sanchez, G. S. Duesberg, N. McEvoy, T. J. Pennycook, C. Downing, A. Crossley, V. Nicolosi and J. N. Coleman, *Nat. Mater.*, 2014, **13**, 624–630.
9 M. Segal, *Nat. Nanotechnol.*, 2009, **4**, 612–614.
10 S. Eigler, M. Enzelberger-Heim, S. Grimm, P. Hofmann, W. Kroener, A. Geworski, C. Dotzer, M. Rockert, J. Xiao, C. Papp, O. Lytken, H. P. Steinrück, P. Müller and A. Hirsch, *Adv. Mater.*, 2013, **25**, 3583–3587.
11 S. Eigler, S. Grimm, M. Enzelberger-Heim, P. Müller and A. Hirsch, *Chem. Commun.*, 2013, **49**, 7391–7393.
12 A. Dimiev, D. V. Kosynkin, L. B. Alemany, P. Chaguine and J. M. Tour, *J. Am. Chem. Soc.*, 2012, **134**, 2815–2822.
13 A. M. Dimiev and J. M. Tour, *ACS Nano*, 2014, **8**, 3060–3068.
14 S. Eigler, S. Grimm and A. Hirsch, *Chem. – Eur. J.*, 2014, **20**, 984–989.
15 S. Eigler, *Phys. Chem. Chem. Phys.*, 2014, **16**, 19832–19835.
16 S. Eigler, F. Hof, M. Enzelberger-Heim, S. Grimm, P. Müller and A. Hirsch, *J. Phys. Chem. C*, 2014, **118**, 7698–7704.
17 G. Charpy, *C. R. Hebd. Séances Acad. Sci.*, 1909, **148**, 920–923.
18 J. William, S. Hummers and R. E. Offeman, *J. Am. Chem. Soc.*, 1958, **80**, 1339.
19 C. K. Chua, A. Ambrosi, Z. Sofer, A. Mackova, V. Havranek, I. Tomandl and M. Pumera, *Chem. – Eur. J.*, 2014, **20**, 15760–15767.
20 C. H. Wong, Z. Sofer, M. Kubesova, J. Kucera, S. Matejkova and M. Pumera, *Proc. Natl. Acad. Sci. U. S. A.*, 2014, **111**, 13774–13779.
21 L. Wang, A. Ambrosi and M. Pumera, *Angew. Chem., Int. Ed.*, 2013, **52**, 13818–13821 (*Angew. Chem.*, 2013, **125**, 14063–14066).
22 A. M. Dimiev, G. Ceriotti, N. Behabtu, D. Zakhidov, M. Pasquali, R. Saito and J. M. Tour, *ACS Nano*, 2013, **7**, 2773–2780.

23 A. M. Dimiev, S. M. Bachilo, R. Saito and J. M. Tour, *ACS Nano*, 2012, **6**, 7842–7849.

24 C. Schafhaeutl, *J. Prakt. Chem.*, 1840, **21**, 129–157.

25 W. Rüdorff and U. Hofmann, *Z. Anorg. Allg. Chem.*, 1938, **238**, 1–50.

26 M. S. Dresselhaus and G. Dresselhaus, *Adv. Phys.*, 2002, **51**, 1–186.

27 T. Enoki, M. Suzuki and M. Endo, *Graphite Intercalation Compounds and Applications*, Oxford University Press, Oxford, 2003.

28 N. I. Kovtyukhova, Y. Wang, A. Berkdemir, R. Cruz-Silva, M. Terrones, V. H. Crespi and T. E. Mallouk, *Nat. Chem.*, 2014, **6**, 957–963.

29 J. Zheng, C. A. Di, Y. Liu, H. Liu, Y. Guo, C. Du, T. Wu, G. Yu and D. Zhu, *Chem. Commun.*, 2010, **46**, 5728–5730.

30 S. Eigler, C. Dotzer, F. Hof, W. Bauer and A. Hirsch, *Chem. – Eur. J.*, 2013, **19**, 9490–9496.

31 L. G. Cançado, A. Jorio, E. H. M. Ferreira, F. Stavale, C. A. Achete, R. B. Capaz, M. V. O. Moutinho, A. Lombardo, T. S. Kulmala and A. C. Ferrari, *Nano Lett.*, 2011, **11**, 3190–3196.

32 S. Chen, W. Cai, R. D. Piner, J. W. Suk, Y. Wu, Y. Ren, J. Kang and R. S. Ruoff, *Nano Lett.*, 2011, **11**, 3519–3525.

33 S. Lee, K. Lee and Z. Zhong, *Nano Lett.*, 2010, **10**, 4702–4707.

34 M. M. Lucchese, F. Stavale, E. H. M. Ferreira, C. Vilani, M. V. O. Moutinho, R. B. Capaz, C. A. Achete and A. Jorio, *Carbon*, 2010, **48**, 1592–1597.